Electronic Supplementary Material (ESI) for Journal of Materials Chemistry A.

Electronic supplementary information

Microwave-Assisted Synthesis of Graphene-like Cobalt Sulfide Freestanding Sheets as an Efficient Bifunctional Electrocatalyst for Overall Water Splitting

Rafai Souleymen[1], Zhitao Wang[1], Chen Qiao[1], Muhammad Naveed[1], and Chuanbao Cao[1]*

[1]Research Center of Materials Science, Beijing Key Laboratory of Construction Tailorable Advanced Functional Materials and Green Applications, Beijing Institute of Technology, Beijing 100081, China.

*Corresponding author E-mail: cbcao@bit.edu.cn

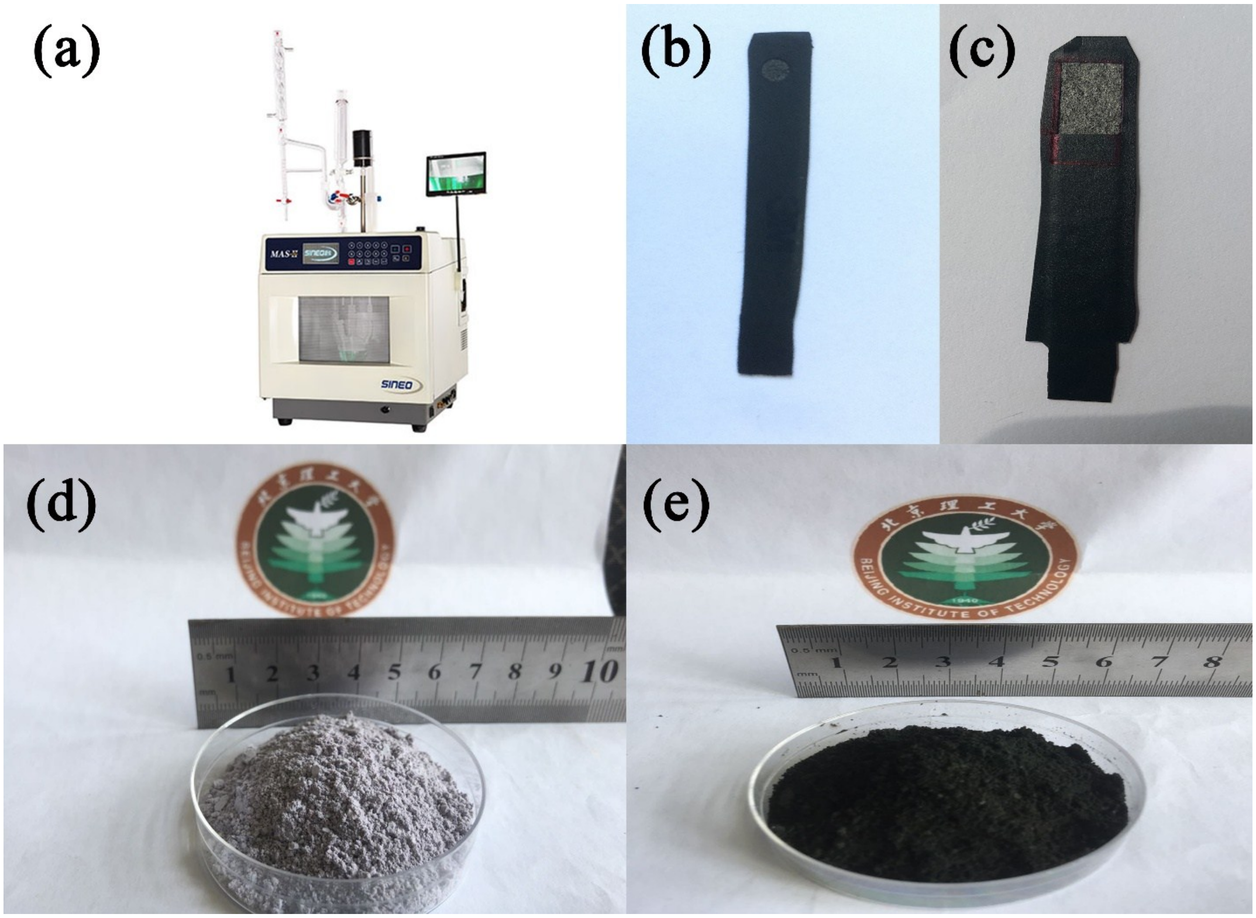

Figure S1. (a) Sineo MAS II+ microwave reactor. (b) A photograph of the as-prepared 3 mm diameter work electrode for HER and OER tests. (c) A photograph of the as-prepared work electrode for the overall water electrolysis S= 0.5 cm × 1 cm. (d) A photograph of a considerable amount of Co(OH)2 freestanding sheets synthesized in one-time reaction. (e) A photograph of a considerable amount of CoSx freestanding sheets synthesized in one-time reaction.

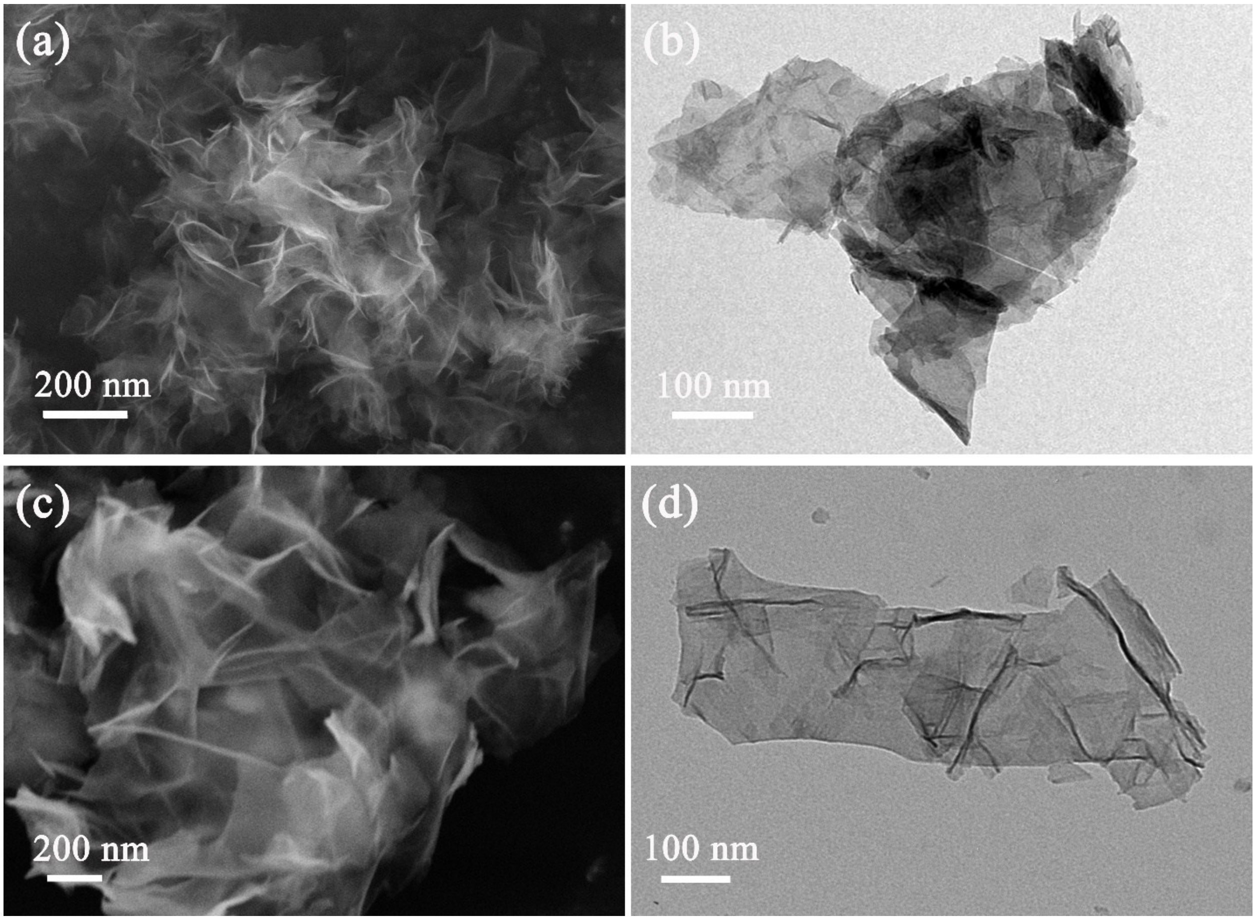

Figure S2. (a, c) SEM images of $Co(OH)_2$ and Co_9S_8 (annealed CoS_x), respectively. (b, d) TEM images of $Co(OH)_2$ and Co_9S_8, respectively.

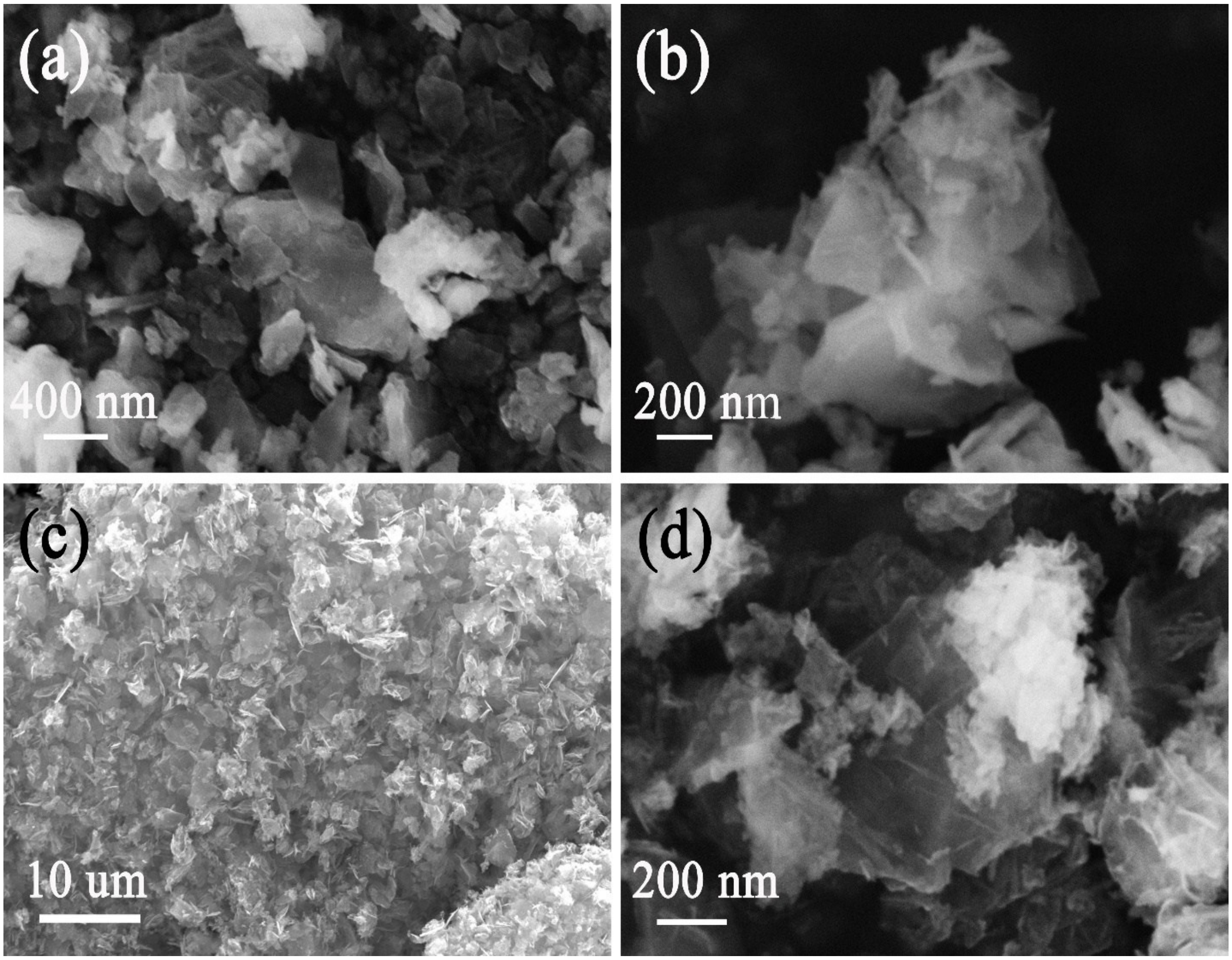

Figure S3. (a, b) SEM images of the CoS_x sheets prepared in pure deionized water as a media for the anion exchange reaction. (c, d) SEM images of CoS_x sheets prepared at 120 °C.

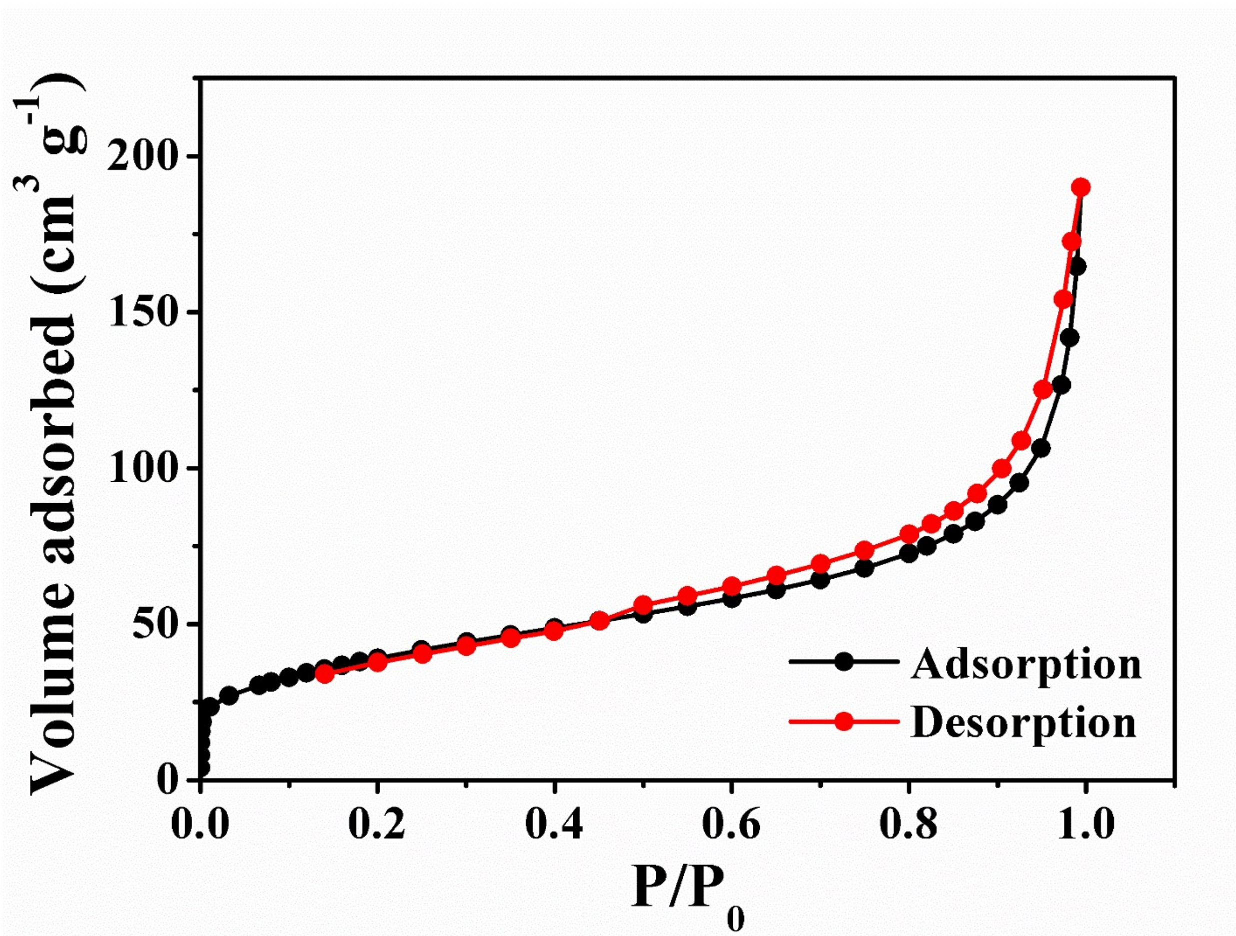

FigureS4. Nitrogen adsorption-desorption isotherms of $Co(OH)_2$ nanosheets. The BET specific surface area of $Co(OH)_2$ nanosheets 140.6 m^2 g^{-1}.

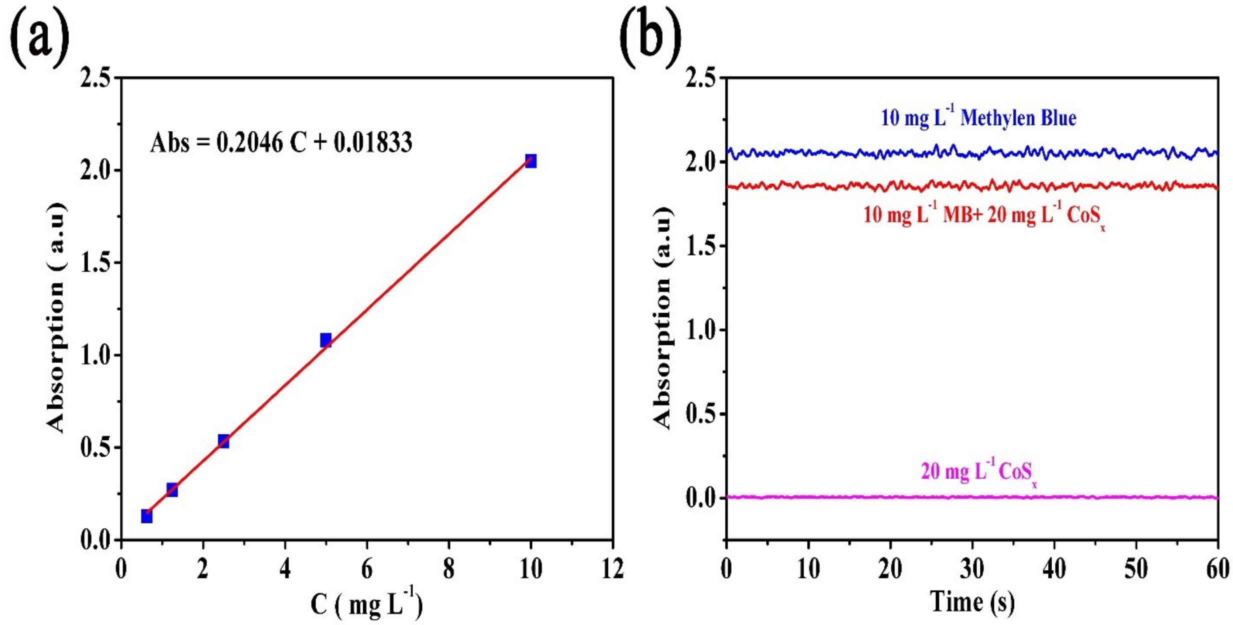

Figure S5. (a) Calibration curve of Methylene Blue (MB) UV-VIS absorption in water solution at λ_{max}= 664 nm. (b) Time-Absorption for 60 s at λ_{max}= 664 nm of 20 mg L^{-1} CoS_x, 10 mg L^{-1} MB, and 10 mg L^{-1} MB + 20 mg L^{-1} CoS_x Solutions.

In the Methylene Blue (MB) absorption technique, the surface area measurements were taken by first preparing standard solutions of MB in water with different concentrations(10 mg, 5 mg, 2.5 mg, 1.25 mg and 0.625 mg) and measure the absorbance of these solutions at λ_{max}= 664 nm. Then, draw a calibration curve (known concentration vs. absorbance) as shown in Figure S5a. The surface area was estimated by adding a known amount of CoS_x sheets (20 mg) to a 1000 ml volumetric flask, a highly enough amount of MB (10 mg) to cover the surface area of the sheets was added and dissolved in 1000 ml of water with stirring, followed by sonication for 2h to fully disperse the agglomerated and stacked CoS_x sheets. Finally, measure the absorbance of the solution at the same λ_{max}= 664 nm and apply to the calibration curve to get the concentration of the remaining MB, the concentration of the remaining MB is about 9.05 mg. The concentration difference with and without dispersing CoS_x is closely related to the amount of the MB molecules adsorbed on the surface of CoS_x sheets. The literature value of 2.54 m^2 of surface covered per 1 mg of MB adsorbed was the basis for our calculations[1], $S = (10\ mg - 9.05\ mg) \times 2.54\ m^2 / 20\ mg = 120.6\ m^2\ g^{-1}$

It is worth noting that a witness solution of bare CoS_x (20 mg in 1000 ml) shows a neutral absorption at λ_{max}= 664 nm (Figure S5b), which confirms that the measured absorption is only due the non-adsorbed MB present in the solution (Figure S5b).

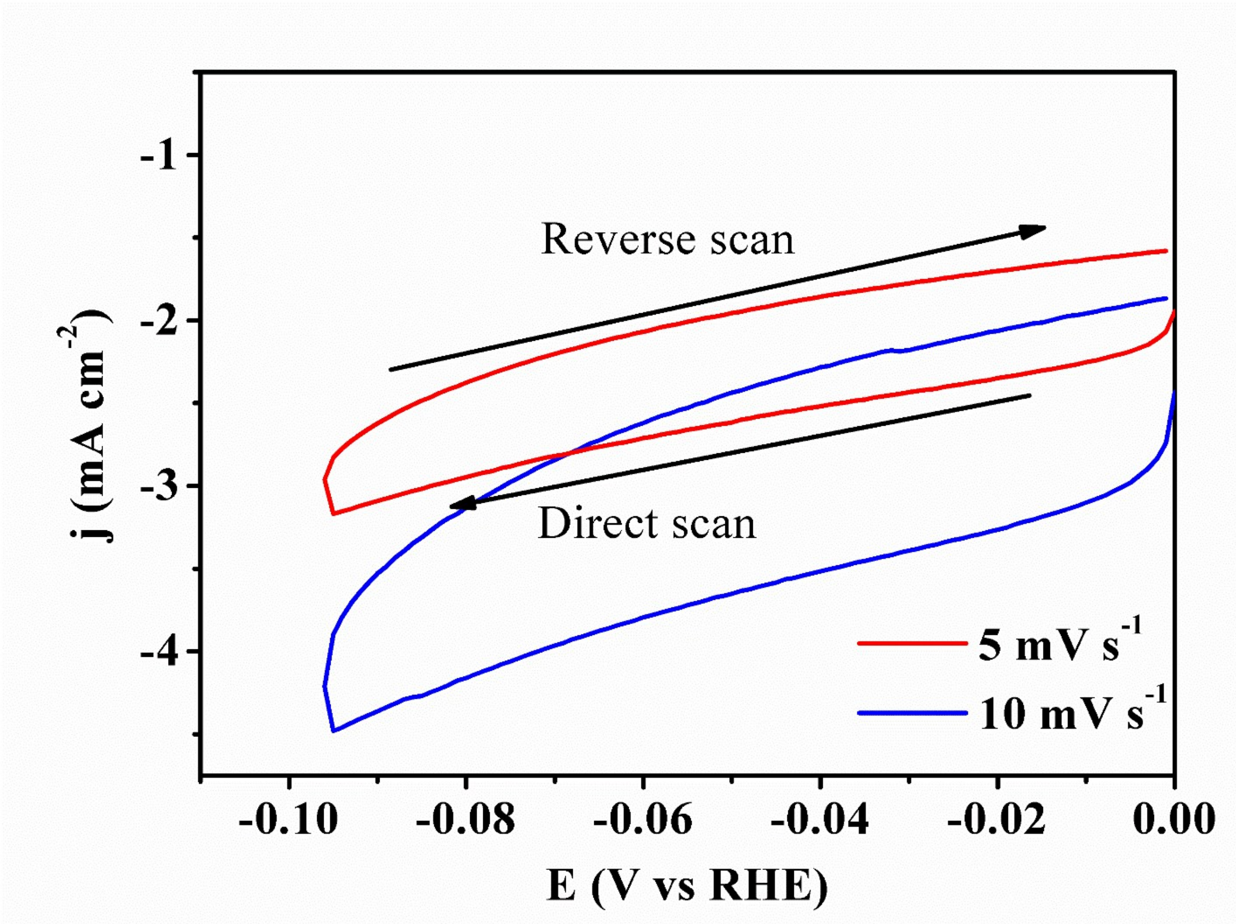

Figure S6. CoS_x cyclic voltammetry at 5 and 10 mV s^{-1} in 1M KOH.

To investigate the nature of the HER cathodic current observed prior 0.1V, cyclic voltammetry was carried out as shown the Figure S6. First, there is no side reaction occurs else than HER as no abnormal oxidation or reduction peak is observed in the CV curve. Secondly, according to the direct scan curve, we notice that CoS_x exhibits an early onset potential for HER lower than 0.02V beyond which the cathode faradic current rises under more negative potentials. Also, the current responses smoothly to the rise of negative potential which imparts that the contribution of non-faradic capacitive current in the collected current is also rather important. In alkaline media, The HER non-faradic current is associated with the strong coverage (double layer) of the adsorbed hydrogen (H_{ads}) formed by the deprotonation of water molecule at the anode surface, making the HER struggle more to move forward further. We have also demonstrated this by the high Tafel slope (123 mV/ decade), indicative of proton adsorption (Volmer step) as the rate-limiting step. Then, we can conclude that the observed background current is a HER current characterized by a slow reaction rate (sluggish kinetics). Thus, a high potential is required to overcome the energy barriers achieve a higher current density of 10 , 20, 50 mA cm^{-2} and so on.

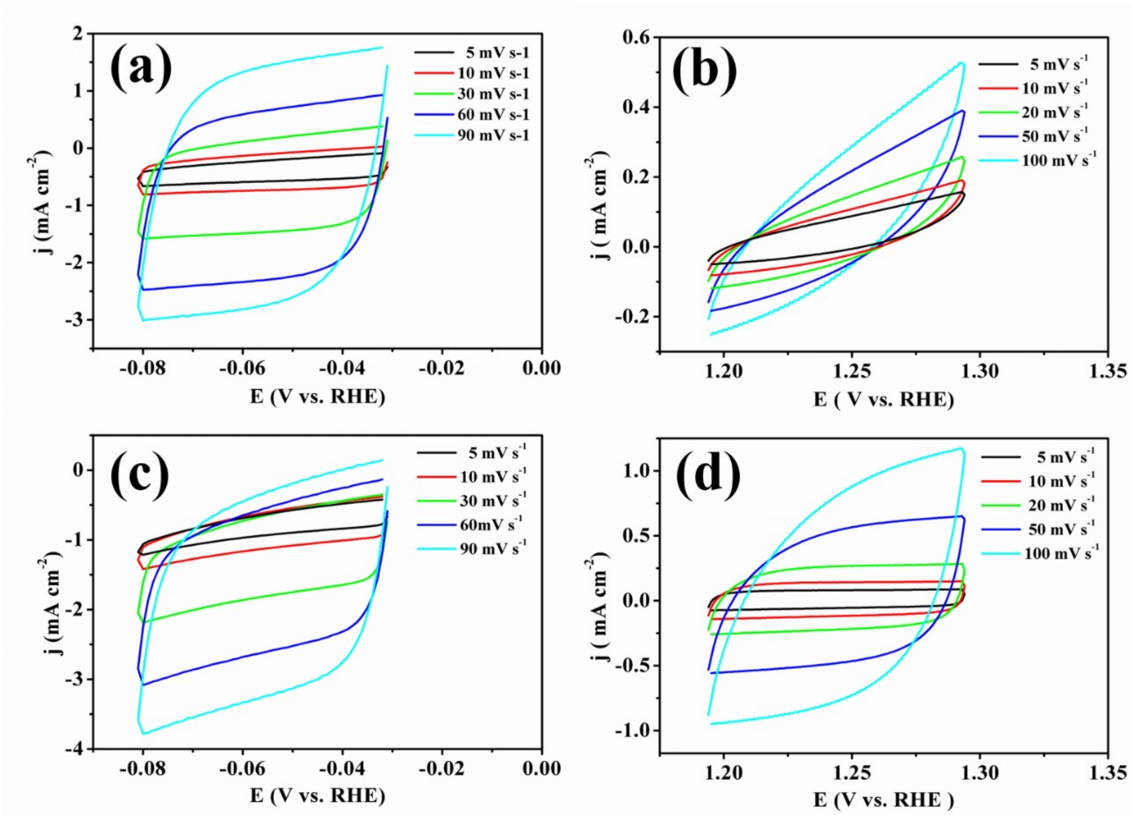

Figure S7. (a,b) CoS_x CV curves at different scan rates in the corresponding HER and OER potential ranges, respectively. (c,d) Co_9S_8 CV curves at different scan rates in the corresponding HER and OER potential ranges, respectively.

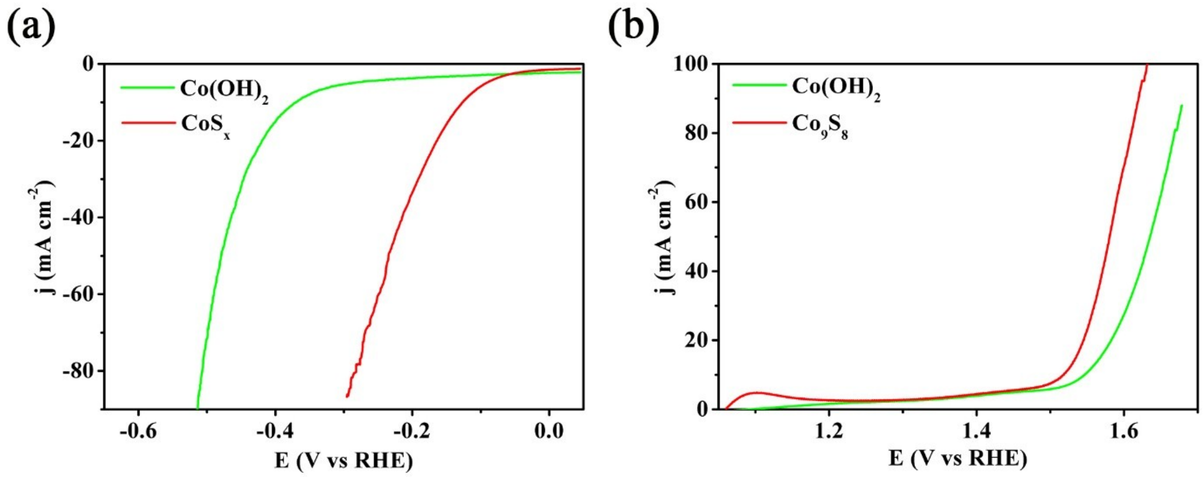

Figure S8. (a) HER polarization curves of $Co(OH)_2$ and CoS_x. (b) OER polarization curves of $Co(OH)_2$ and Co_9S_8.

Table S1. Comparison of the HER performances of CoSx with the best reported cobalt sulfide-based HER electrocatalysts.

Catalyst	Morphology	Electrolyte	Overpotential η_{10} (mV)	Tafel Slope (mV dec^{-1})	Ref
CoS_x	Freestanding sheets	1M KOH	127(10mA cm^{-2}) 187(20mA cm^{-2}) 240(50mA cm^{-2})	123	This work
Co-S/CP Co-S/CTs/CP	Nanosheets	1M KOH	357 190	138 131	2
Co_9S_8@CNFs	Octahedron	1M KOH	>400	203	3
Co_3S_4	Polyhedrons	1M KOH 0.5M H_2SO_4	290 380	85.3 _	4
CoS_2	Pyramids(film)	1M KOH 0.5M H_2SO_4	244 190	72 133	5
Co_9S_8@C	Nanoparticles	1M KOH 0.5M H_2SO_4	250 240	– _	6
MW-CoS ST-CoS	Nanoprisms	phosphate buffer pH=7	275 298	75 90	7
CoS_2/RGO CoS_2/RGO/CNT	Nanosheets	0.5M H_2SO_4	280 142	82 51	8
CoS_2	Nanowires	0.5M H_2SO_4	145	51.6	9

CoS_2	Film	0.5M H_2SO_4	190	52	10

Table S2. Comparison of the HER performances of CoS_x with other reported non-precious HER electrocatalysts.

Catalyst	Morphology	Electrolyte	Overpotential η_{10} (mV)	Tafel Slope (mV dec^{-1})	Ref
CoS_x	Free standing Nanosheets	1M KOH	127(10mA cm^{-2}) 187(20mA cm^{-2}) 240(50mA cm^{-2})	123	This work
Ni_3S_2	Nanosheet/Ni Foam	1M KOH	223	_	11
Ni_3S_2	Nanoparticles/CNTs	1M KOH	480	102	12
$Ni_{0.33}Co_{0.67}S_2$/Ti foil	Nanowires	1MKOH	88	118	13
$NiSe_2$	Nanosheets	1M KOH	184	184	14
Co_9S_8@MoS_2	Octahedrons /CNFs	1M KOH	190	110	3
CoP	Nanowires/CC	1M KOH	110	129	15
CoP	Film	1M KOH	94	42	16
CoN_x/C	NPs/porous carbon	1M KOH	170	75	17
MoS_2-Ni_3S_2	Nanorods/Ni foam	1M KOH	98	61	18
NiP	Nanoplates	1M KOH	160 (20 mA cm^{-2})	107	19
NiMnCoS@rGO	Nanoparticules@sheets	1M KOH	150	52	20
Co@N-C	Nanoparticules	1M KOH	210	108	21
Co-Ni@NC	Nanospheres	1M KOH	180	193	22
CoO_x@CN	Nanoparticules@sheets	1M KOH	232	115	23
CoPS	Nanoplates/CFP	0.5 H_2SO_4	48	56	24
MoS_2/$CoSe_2$	Nanosheets/nanobetls	0.5 H_2SO_4	68	39	25
MoS_2	Film	0.5 H_2SO_4	260	50	26

WS_2	Nanosheets	0.5 H_2SO_4	250	60	[27]
Ni-$CoSe_2$	NPs-nanobelts	0.5 H_2SO_4	90	39	[28]

Table S3. Comparison of the OER performance of CoS_x with other reported cobalt sulfide-based HER electrocatalysts.

Catalyst	Morphology	Electrolyte	Overpotential η_{10} (mV)	Tafel slope ($mVdec^{-1}$)	Ref
Co_9S_8	Freestanding nanosheets	1M KOH	288	79	This work
Co_3S_4	Nanosheets	1M KOH	363	90	[29]
Co_3S_4	Nanosheets	1M KOH	>470	144	[30]
Co_9S_8 $Co_{1-x}S$	Hollow microplates	1M KOH	278 300	53 53.7	[31]
Co-S/Ti mesh	Nanosheets	1M KOH	361	64	[32]
Co_3S_4@N,S-rGO	NPs@naosheets	0.1M KOH	375	_	[33]
Co-S/CP Co-S/CTs/CP	Nanosheets	1M KOH	363 306	101 72	[2]
Co_9S_8@CNFs	Octahedron	1M KOH	512	78	[3]
CoxSy@N, S- C	NPs@Porous C	1M KOH	470	_	[34]

Table S4. Comparison of the OER performances of Co_9S_8 with other reported non-precious HER electrocatalysts.

Catalyst	Morphology	Electrolyte	Overpotential η_{10} (mV)	Tafel slope (mV dec^{-1})	Ref
Co_9S_8	Freestanding nanosheets	1M KOH	288	79	This work
$CuCo_2S_4$	Nanosheets	1M KOH	310	86	[30]
$Zn_{0.76}Co_{0.24}S/CoS_2$	Nanowires	1M KOH	>316	79	[35]
Co_9S_8@MoS_2	Octahedrons/CNFs	1M KOH	430	61	[3]
NiFe LDH	Nanoplates	1M KOH	302	40	[36]
CoMn LDH	Nanoplates	1M KOH	324	43	[37]
Co_5MnLDH/MWCNT	Nanosheets/MWCNT	1M KOH	300	73.6	[38]
MoS_2-Ni_3S_2/NF	Nanorods/Ni foam	1M KOH	249	66	[18]
$(Ni, Co)_{0.85}Se$@CC	Nanotubes/CC	1M KOH	255	79	[39]
CoCr LDH	Nanosheets	1M NaOH	340	81	[40]
$Ni(OH)_2$	Nanosheets/Ni faom	1M KOH	170	150	[41]
Ni_xP_y	Nanoplates	1M KOH	320	72.2	[19]
$Zn_{4-x}Co_xSO_4(OH)_6\cdot 0.5H_2O$	Nanoplates	0.5M KOH	370	60	[42]
$NiMnCoO_x$@rGO	Nanoparticules@sheets	1M KOH	320	53	[20]

Table S5. Comparison of overall water splitting performance of CoS_xIICo_9S_8 with recently reported bi-functional electrocatalysts in basic electrolyte.

Cathode catalyst	Anode catalyst	Electrolyte	HER η10 (mV)	OER η10 (mV)	E at j = 10 mA cm^{-2} (V)	Ref
CoS_x	Co_9S_8	1M KOH	127	288	1.55 (20 mA cm^{-2})	This work
Co-S/CTs/CP	Co-S/CTs/CP	1M KOH	190	306	1.74	[2]
MoS2-Ni3S/Ni foam	MoS2-Ni3S/Ni foam	1M KOH	90	249	1.50	[18]
Ni_2P/Ni/Ni Foam	Ni_2P/Ni/Ni foam	1M KOH	90	200	1.49	[43]
Ni_xP_y	Ni_xP_y	1M KOH	160 (20 mA cm^{-2})	320	1.57	[19]
NiS/Ni foam	Ni/Ni Foam	1M KOH	158 (20 mA cm^{-2})	355 (50 mA cm^{-2})	1.67	[44]
$NiMnCoS_x$@rGO	$NiMnCoO_x$@rGO	1M KOH	150	320	1.56 (20 mA cm^{-2})	[20]
$Ni(OH)_2$/Ni foam	$Ni(OH)_2$/Ni foam	1M KOH	178 (20 mA cm^{-2})	330 (50 mA cm^{-2})	1.68	[41]
$Ni_{0.33}Co_{0.67}S_2$/Ti foil	$Ni_{0.33}Co_{0.67}O_2$/Ti foil	1M KOH	88	>330 (onset)	1.73	[13]

Notes and references

(1) McAllister, M. J.; Li, J. L.; Adamson, D. H.; Schniepp, H. C.; Abdala, A. A.; Liu, J.;

Herrera-Alonso, M.; Milius, D. L.; Car, R.; Prud'homme, R. K.; *et al.* Single Sheet Functionalized Graphene by Oxidation and Thermal Expansion of Graphite. *Chem. Mater.* **2007**, *19*, 4396–4404.

(2) Wang, J.; Zhong, H.; Wang, Z.; Meng, F.; Zhang, X. Integrated Three-Dimensional Carbon Paper/carbon Tubes/cobalt-Sulfide Sheets as an Efficient Electrode for Overall Water Splitting. *ACS Nano* **2016**, *10*, 2342–2348.

(3) Zhu, H.; Zhang, J.; Yanzhang, R.; Du, M.; Wang, Q.; Gao, G.; Wu, J.; Wu, G.; Zhang, M.; Liu, B.; *et al.* When Cubic Cobalt Sulfide Meets Layered Molybdenum Disulfide: A Core-Shell System Toward Synergetic Electrocatalytic Water Splitting. *Adv. Mater.* **2015**, *27*, 4752–4759.

(4) Huang, Z. F.; Song, J.; Li, K.; Tahir, M.; Wang, Y. T.; Pan, L.; Wang, L.; Zhang, X.; Zou, J. J. Hollow Cobalt-Based Bimetallic Sulfide Polyhedra for Efficient All-pH-Value Electrochemical and Photocatalytic Hydrogen Evolution. *J. Am. Chem. Soc.* **2016**, *138*, 1359–1365.

(5) Zhang, H.; Li, Y.; Zhang, G.; Wan, P.; Xu, T.; Wu, X.; Sun, X. Highly Crystallized Cubic Cattierite CoS2 for Electrochemically Hydrogen Evolution over Wide pH Range from 0 to 14. *Electrochim. Acta* **2014**, *148*, 170–174.

(6) Feng, L. L.; Li, G. D.; Liu, Y.; Wu, Y.; Chen, H.; Wang, Y.; Zou, Y. C.; Wang, D.; Zou, X. Carbon-Armored Co9S8 Nanoparticles as All-pH Efficient and Durable H2-Evolving Electrocatalysts. *ACS Appl. Mater. Interfaces* **2015**, *7*, 980–988.

(7) You, B.; Jiang, N.; Sheng, M.; Sun, Y. Microwave vs. Solvothermal Synthesis of Hollow

Cobalt Sulfide Nanoprisms for Electrocatalytic Hydrogen Evolution and Supercapacitors. *Chem. Commun.* **2015**, *51*, 4252–4255.

(8) Peng, S.; Li, L.; Han, X.; Sun, W.; Srinivasan, M.; Mhaisalkar, S. G.; Cheng, F.; Yan, Q.; Chen, J.; Ramakrishna, S. Cobalt Sulfide Nanosheet/graphene/carbon Nanotube Nanocomposites as Flexible Electrodes for Hydrogen Evolution. *Angew. Chemie* **2014**, *126*, 12802–12807.

(9) Faber, M. S.; Dziedzic, R.; Lukowski, M. A.; Kaiser, N. S.; Ding, Q.; Jin, S. High-Performance Electrocatalysis Using Metallic Cobalt Pyrite (CoS 2) Micro- and Nanostructures. *J. Am. Chem. Soc.* **2014**, *136*, 10053–10061.

(10) Faber, M. S.; Lukowski, M. A.; Ding, Q.; Kaiser, N. S.; Jin, S. Earth-Abundant Metal Pyrites (FeS2, CoS2, NiS2, and Their Alloys) for Highly Efficient Hydrogen Evolution and Polysulfide Reduction Electrocatalysis. *J. Phys. Chem. C* **2014**, *118*, 21347–21356.

(11) Feng, L. L.; Yu, G.; Wu, Y.; Li, G. D.; Li, H.; Sun, Y.; Asefa, T.; Chen, W.; Zou, X. High-Index Faceted Ni3S2 Nanosheet Arrays as Highly Active and Ultrastable Electrocatalysts for Water Splitting. *J. Am. Chem. Soc.* **2015**, *137*, 14023–14026.

(12) Lin, T. W.; Liu, C. J.; Dai, C. S. Ni3S2/carbon Nanotube Nanocomposite as Electrode Material for Hydrogen Evolution Reaction in Alkaline Electrolyte and Enzyme-Free Glucose Detection. *Appl. Catal. B Environ.* **2014**, *154–155*, 213–220.

(13) Zheng, G.; Peng, Z.; Jia, D.; Al-Enizi, A. M.; Elzatahry, A. A. From Water Oxidation to Reduction: Homologous Ni-Co Based Nanowires as Complementary Water Splitting Electrocatalysts. *Adv. Energy Mater.* **2015**, *5*, 1–7.

(14) Liang, H.; Li, L.; Meng, F.; Dang, L.; Zhuo, J.; Forticaux, A.; Wang, Z.; Jin, S. Porous Two-Dimensional Nanosheets Converted from Layered Double Hydroxides and Their Applications in Electrocatalytic Water Splitting. *Chem. Mater.* **2015**, *27*, 5702–5711.

(15) Tian, J.; Liu, Q.; Asiri, A. M.; Sun, X. Self-Supported Nanoporous Cobalt Phosphide Nanowire Arrays: An Efficient 3D Hydrogen-Evolving Cathode over the Wide Range of pH 0-14. *J. Am. Chem. Soc.* **2014**, *136*, 7587–7590.

(16) Jiang, N.; You, B.; Sheng, M.; Sun, Y. Electrodeposited Cobalt-Phosphorous-Derived Films as Competent Bifunctional Catalysts for Overall Water Splitting. *Angew. Chemie - Int. Ed.* **2015**, *54*, 6251–6254.

(17) Liang, H.-W.; Brüller, S.; Dong, R.; Zhang, J.; Feng, X.; Müllen, K. Molecular metal–Nx Centres in Porous Carbon for Electrocatalytic Hydrogen Evolution. *Nat. Commun.* **2015**, *6*, 7992.

(18) Yang, Y.; Zhang, K.; Lin, H.; Li, X.; Chan, H. C.; Yang, L.; Gao, Q. Heteronanorods of MoS2-Ni3S2 as Efficient and Stable Bi-Functional Electrocatalysts for Overall Water Splitting. *ACS Catal.* **2017**, acscatal.6b03192.

(19) Li, J.; Li, J.; Zhou, X.; Xia, Z.; Gao, W.; Ma, Y.; Qu, Y. Highly Efficient and Robust Nickel Phosphides as Bifunctional Electrocatalysts for Overall Water-Splitting. *ACS Appl. Mater. Interfaces* **2016**, *8*, 10826–10834.

(20) Miao, R.; He, J.; Sahoo, S.; Luo, Z.; Zhong, W.; Chen, S.-Y.; Guild, C.; Jafari, T.; Dutta, B.; Cetegen, S. A.; *et al.* Reduced Graphene Oxide Supported Nickel–Manganese–Cobalt Spinel Ternary Oxide Nanocomposites and Their Chemically Converted Sulfide

Nanocomposites as Efficient Electrocatalysts for Alkaline Water Splitting. *ACS Catal.* **2017**, *7*, 819–832.

(21) Wang, J.; Gao, D.; Wang, G.; Miao, S.; Wu, H.; Li, J.; Bao, X. Cobalt Nanoparticles Encapsulated in Nitrogen-Doped Carbon as a Bifunctional Catalyst for Water Electrolysis. *J. Mater. Chem. A* **2014**, *2*, 20067–20074.

(22) Deng, J.; Ren, P.; Deng, D.; Bao, X. Enhanced Electron Penetration through an Ultrathin Graphene Layer for Highly Efficient Catalysis of the Hydrogen Evolution Reaction. *Angew. Chemie - Int. Ed.* **2015**, *54*, 2100–2104.

(23) Jin, H.; Wang, J.; Su, D.; Wei, Z.; Pang, Z.; Wang, Y. In Situ Cobalt-Cobalt oxide/N-Doped Carbon Hybrids as Superior Bifunctional Electrocatalysts for Hydrogen and Oxygen Evolution. *J. Am. Chem. Soc.* **2015**, *137*, 2688–2694.

(24) Cabán-Acevedo, M.; Stone, M. L.; Schmidt, J. R.; Thomas, J. G.; Ding, Q.; Chang, H.-C.; Tsai, M.-L.; He, J.-H.; Jin, S. Efficient Hydrogen Evolution Catalysis Using Ternary Pyrite-Type Cobalt Phosphosulphide. *Nat. Mater.* **2015**, *14*, 1245–1251.

(25) Gao, M.-R.; Liang, J.-X.; Zheng, Y.-R.; Xu, Y.-F.; Jiang, J.; Gao, Q.; Li, J.; Yu, S.-H. An Efficient Molybdenum Disulfide/cobalt Diselenide Hybrid Catalyst for Electrochemical Hydrogen Generation. *Nat. Commun.* **2015**, *6*, 5982.

(26) Kibsgaard, J.; Chen, Z.; Reinecke, B. N.; Jaramillo, T. F. Engineering the Surface Structure of MoS2 to Preferentially Expose Active Edge Sites for Electrocatalysis. *Nat. Mater.* **2012**, *11*, 963–969.

(27) Voiry, D.; Yamaguchi, H.; Li, J.; Silva, R.; Alves, D. C. B.; Fujita, T.; Chen, M.; Asefa,

T.; Shenoy, V. B.; Eda, G.; *et al.* Enhanced Catalytic Activity in Strained Chemically Exfoliated WS2 Nanosheets for Hydrogen Evolution. *Nat. Mater.* **2013**, *12*, 850–855.

(28) Xu, Y. F.; Gao, M. R.; Zheng, Y. R.; Jiang, J.; Yu, S. H. Nickel/nickel(II) Oxide Nanoparticles Anchored onto cobalt(IV) Diselenide Nanobelts for the Electrochemical Production of Hydrogen. *Angew. Chemie - Int. Ed.* **2013**, *52*, 8546–8550.

(29) Zhao, W.; Zhang, C.; Geng, F.; Zhuo, S.; Zhang, B. Nanoporous Hollow Transition Metal Chalcogenide Nanosheets Synthesized via the Anion-Exchange Reaction of Metal Hydroxides with Chalcogenide Ions. *ACS Nano* **2014**, *8*, 10909–10919.

(30) Chauhan, M.; Reddy, K. P.; Gopinath, C. S.; Deka, S. Copper Cobalt Sulfide Nanosheets Realizing a Promising Electrocatalytic Oxygen Evolution Reaction. *ACS Catal.* **2017**, 5871–5879.

(31) Liu, H.; Ma, F.-X.; Xu, C.-Y.; Yang, L.; Du, Y.; Wang, P.-P.; Yang, S.; Zhen, L. Sulfurizing-Induced Hollowing of Co_9S_8 Microplates with Nanosheet Units for Highly Efficient Water Oxidation. *ACS Appl. Mater. Interfaces* **2017**, *9*, 11634–11641.

(32) Liu, T.; Liang, Y.; Liu, Q.; Sun, X.; He, Y.; Asiri, A. M. Electrodeposition of Cobalt-Sulfide Nanosheets Film as an Efficient Electrocatalyst for Oxygen Evolution Reaction. *Electrochem. commun.* **2015**, *60*, 92–96.

(33) Liu, Q.; Jin, J.; Zhang, J. NiCo2S4@graphene as a Bifunctional Electrocatalyst for Oxygen Reduction and Evolution Reactions. *ACS Appl. Mater. Interfaces* **2013**, *5*, 5002–5008.

(34) Chen, B.; Li, R.; Ma, G.; Gou, X.; Zhu, Y.; Xia, Y. Cobalt sulfide/N,S Codoped Porous

Carbon Core–shell Nanocomposites as Superior Bifunctional Electrocatalysts for Oxygen Reduction and Evolution Reactions. *Nanoscale* **2015**, *7*, 20674–20684.

(35) Liang, Y.; Liu, Q.; Luo, Y.; Sun, X.; He, Y.; Asiri, A. M. Zn0.76Co0.24S/CoS2 Nanowires Array for Efficient Electrochemical Splitting of Water. *Electrochim. Acta* **2016**, *190*, 360–364.

(36) Song, F.; Hu, X. Exfoliation of Layered Double Hydroxides for Enhanced Oxygen Evolution Catalysis. **2014**.

(37) Song, F.; Hu, X. Ultrathin Cobalt-Manganese Layered Double Hydroxide Is an Efficient Oxygen Evolution Catalyst. *J. Am. Chem. Soc.* **2014**, *136*, 16481–16484.

(38) Jia, G.; Hu, Y.; Qian, Q.; Yao, Y.; Zhang, S.; Li, Z.; Zou, Z. Formation of Hierarchical Structure Composed of (Co/Ni)Mn-LDH Nanosheets on MWCNT Backbones for Efficient Electrocatalytic Water Oxidation. *ACS Appl. Mater. Interfaces* **2016**, *8*, 14527–14534.

(39) Xia, C.; Jiang, Q.; Zhao, C.; Hedhili, M. N.; Alshareef, H. N. Selenide-Based Electrocatalysts and Scaffolds for Water Oxidation Applications. *Adv. Mater.* **2016**, *28*, 77–85.

(40) Dong, C.; Yuan, X.; Wang, X.; Liu, X.; Dong, W.; Wang, R.; Duan, Y.; Huang, F. Rational Design of Cobalt–chromium Layered Double Hydroxide as a Highly Efficient Electrocatalyst for Water Oxidation. *J. Mater. Chem. A* **2016**, *4*, 11292–11298.

(41) Rao, Y.; Wang, Y.; Ning, H.; Li, P.; Wu, M. Hydrotalcite-like $Ni(OH)_2$ Nanosheets in Situ Grown on Nickel Foam for Overall Water Splitting. *ACS Appl. Mater. Interfaces*

2016, *8*, 33601–33607.

(42) Dutta, S.; Ray, C.; Negishi, Y.; Pal, T. Facile Synthesis of Unique Hexagonal Nanoplates of Zn/Co Hydroxy Sulfate for Efficient Electrocatalytic Oxygen Evolution Reaction. *ACS Appl. Mater. Interfaces* **2017**, *9*, 8134–8141.

(43) You, B.; Jiang, N.; Sheng, M.; Bhushan, M. W.; Sun, Y. Hierarchically Porous Urchin-Like Ni2P Superstructures Supported on Nickel Foam as Efficient Bifunctional Electrocatalysts for Overall Water Splitting. *ACS Catal.* **2016**, *6*, 714–721.

(44) Zhu, W.; Yue, X.; Zhang, W.; Yu, S.; Zhang, Y.; Wang, J.; Wang, J. Nickel Sulfide Microsphere Film on Ni Foam as an Efficient Bifunctional Electrocatalyst for Overall Water Splitting. *Chem. Commun.* **2016**, *52*, 1486–1489.